Nonadiabatic corrections to elastic scattering of halo nuclei

N. C. Summers,* J. S. Al-Khalili, and R. C. Johnson
Department of Physics, School of Physics and Chemistry, University of Surrey, Guildford, Surrey GU2 7XH, United Kingdom
(Received 26 April 2002; published 24 July 2002)

We derive the formalism for the leading order corrections to the adiabatic approximation to the scattering of composite projectiles. Assuming a two-body projectile of core plus loosely bound valence particle and a model (the core recoil model) in which the interaction of the valence particle and the target can be neglected, we derive the nonadiabatic correction terms both exactly, using a partial wave analysis, and using the eikonal approximation. Along with the expected energy dependence of the corrections, there is also a strong dependence on the valence-to-core mass ratio and on the strength of the imaginary potential for the core-target interaction, which relates to absorption of the core in its scattering by the target. The strength and diffuseness of the core-target potential also determine the size of the corrections. The first order nonadiabatic corrections were found to be smaller than qualitative estimates would expect. The large absorption associated with the core-target interaction in such halo nuclei as ^{11}Be kills off most of the nonadiabatic corrections. We give an improved estimate for the range of validity of the adiabatic approximation when the valence-target interaction is neglected, which includes the effect of core absorption. Some consideration was given to the validity of the eikonal approximation in our calculations.

DOI: 10.1103/PhysRevC.66.014614 PACS number(s): 24.10.−i, 21.45.+v, 25.60.Bx

I. INTRODUCTION

Halo nuclei are often described by few-body models which recognize selected internal degrees of freedom of the nucleus. Few-body reaction models assume the projectile nucleus consists of core and valence clusters, which interact with the target while also interacting with each other. Using this few-body approach, excitations of the projectile to both bound and continuum states may be included within the reaction model; this breakup is significant for weakly bound systems, such as halo nuclei. Further approximations are usually necessary to handle the breakup continuum.

One such approach which includes strong couplings to the continuum is the adiabatic approximation [1], in which the breakup continuum is collapsed onto a single channel which is degenerate with the ground state of the projectile. This is often referred to in the Coulomb excitation literature as the sudden approximation. Another approach to solving the few-body problem, without requiring the use of the adiabatic approximation, is the coupled discretized continuum channel (CDCC) method. Here, convergence of the observables may be obtained in most cases without the need for further approximations. CDCC methods, in which the breakup continuum is truncated and discretized, have been effectively applied to reactions involving two-body projectiles, such as deuterons and single neutron halo nuclei. However, the adiabatic approach provides a simpler calculation scheme and, as yet, is the only method for dealing with multichannel effects, including the continuum, for three-body projectiles. Three-body models are frequently used for two-neutron halos such as ^{6}He, ^{11}Li, and ^{14}Be.

A special case of the adiabatic model is when the interaction between the core and the target dominates and the interaction between the valence particle and the target can be neglected [2]; we call this the *core recoil model*, since the only way the projectile can be excited is through recoil of the core in its scattering by the target. This has been applied to the elastic scattering of halo nuclei, such as ^{11}Be, where the core-to-valence mass ratio is large [2]. The core recoil model is also particularly applicable to a Coulomb dominated process when the valence particle is neutral, and has been applied to the Coulomb breakup of high energy deuterons [3,4] and for one and two neutron halos [5,6].

With the current interest in radioactive nuclear beams operating at energies in the region of tens of MeVs, the validity of high energy models, such as the adiabatic model, at lower energies is of importance. Comparisons of CDCC and adiabatic methods for deuteron induced reactions have been extensively studied [7]. The adiabatic model was shown to be accurate at much lower energies than one would expect from qualitative estimates based on the basic assumption of the adiabatic approximation—that the breakup energies of the projectile excited during the reaction are small relative to the center of mass energy of the projectile. A simple estimate of the accuracy of the adiabatic approximation for elastic scattering and elastic breakup is given in Ref. [8] within the core recoil model. However, this estimate did not take into consideration processes such as core absorption, which has been suggested as an important factor in improving the accuracy of the adiabatic approximation [7].

The adiabatic approximation underlies many microscopic theories of nuclear reactions, such as Glauber theory [9]. Glauber models have been extensively applied to reactions involving deuterons and light halo nuclei [10,11] and have been useful for extracting information on halo sizes due to their diffuse nature [12,13]. Much work has gone into correcting the eikonal assumptions made in Glauber theory [14,15]. Corrected calculations compare well to few-body calculations which make only the adiabatic approximation, based on the method of Refs. [16–18].

*Electronic address: n.summers@surrey.ac.uk

The formulas for the leading order nonadiabatic corrections in the core recoil model were given first in Ref. [19]. This paper derived the leading order corrections using the eikonal approximation, and discussed the relevance of the terms involved. Here, we calculate these corrections for ^{11}Be and ^{6}He elastic scattering from a ^{12}C target at 10 MeV/nucleon. The nonadiabatic corrections were found to be identically zero for a pure point Coulomb potential [19]. The cross terms for the case of nuclear+Coulomb interactions are also small for light ion reactions [20]. The accuracy of the adiabatic approximation for small angle Coulomb scattering was discussed in Ref. [8]. In this paper, all Coulomb effects are ignored. It is felt that this provides an adequate framework for discussing the validity of the adiabatic approximation, although no comparison with experimental data is possible. A full comparison of the adiabatic approximation with experimental data, for the elastic scattering of a single neutron halo, including Coulomb effects, has been made in Ref. [2].

The format of the paper is as follows. In Sec. II we discuss the adiabatic approximation in the special case of the core recoil model, where the valence-target interaction is neglected. The validity of the adiabatic approximation in the core recoil model is examined using qualitative arguments, and comparisons with CDCC calculations are made. In Sec. III we rederive the formulas in Ref. [19] using an alternative method which expresses the internal Hamiltonian operator for the projectile as the product of two operators. We provide an eikonal derivation as in Ref. [19] and then derive the corrections exactly using a partial wave sum. The eikonal approximation provides useful insights into the nature of the nonadiabatic corrections while the exact calculation is used to examine the range of validity of the eikonal approximation to the corrections. This provides some justification for the use of the eikonal approximation in more complete calculations which include the valence-target interaction. These will be reported elsewhere [20,21]. In Sec. IV, we present calculations of the nonadiabatic correction in the core recoil model for ^{11}Be and ^{6}He. Section V gives an improved estimate for the range of validity for the adiabatic approximation. A summary and concluding remarks are given in Sec. VI.

II. ADIABATIC APPROXIMATION

Here we describe the projectile using a two-body model. The position of the valence particle (v) relative to the core (c) is described by the vector $\boldsymbol{r}$. The position vector of the center of mass of the whole projectile from the target is $\boldsymbol{R}$. The few-body Hamiltonian is

$$H = T_{\boldsymbol{R}} + V_{cT}(\boldsymbol{R} - \alpha \boldsymbol{r}) + V_{vT}(\boldsymbol{R} - \beta \boldsymbol{r}) + H_{vc}, \tag{1}$$

where

$$T_{\boldsymbol{R}} = \hbar^2 K_R^2 / 2\mu, \quad \mathrm{i}\boldsymbol{K}_{\boldsymbol{R}} = \boldsymbol{\nabla}_{\boldsymbol{R}}, \tag{2}$$

$$H_{vc} = \hbar^2 K_r^2 / 2\mu_{vc} + V_{vc}(\boldsymbol{r}), \quad \mathrm{i}\boldsymbol{K}_{\boldsymbol{r}} = \boldsymbol{\nabla}_{\boldsymbol{r}}. \tag{3}$$

Here, H_{vc} is the internal Hamiltonian of the projectile which has a ground state wave function, ϕ_0, satisfying

$$(H_{vc} + \varepsilon_0)\phi_0 = 0, \tag{4}$$

where ε_0 is the binding energy of the projectile. The core-target and valence-target potentials are V_{cT} and V_{vT}, respectively, while V_{vc} is the core-valence potential that binds the projectile. The reduced masses of the projectile-target and core-valence systems are μ and μ_{vc}, respectively, while the mass ratios $\alpha = m_v/m_P$ and $\beta = -m_c/m_P = \alpha - 1$ relate to the distance of the core and valence clusters from the center of mass of the projectile.

The exact wave function for the few-body scattering system is [22]

$$|\Psi_{\boldsymbol{K}}^{(+)}\rangle = \frac{\mathrm{i}\epsilon}{E^+ - H}|\phi_0, \boldsymbol{K}\rangle, \tag{5}$$

$$E^+ = E + \mathrm{i}\epsilon, \quad \epsilon \to 0^+, \tag{6}$$

where E is the total energy of the few-body scattering system and $\boldsymbol{K}$ is the center-of-mass momentum. The adiabatic approximation [1] assumes that the internal motion of the projectile is frozen, and thus the internal Hamiltonian of the projectile can be replaced by a constant. This is chosen to be the ground state energy of the projectile ($-\varepsilon_0$), because then the incident part of the three-body wave function has unit amplitude. The adiabatic wave function is therefore

$$|\Psi_{\boldsymbol{K}}^{\mathrm{ad}(+)}\rangle = \frac{\mathrm{i}\epsilon}{E_0^+ - T_{\boldsymbol{R}} - V_{cT} - V_{vT}}|\phi_0, \boldsymbol{K}\rangle, \tag{7}$$

where $E_0 = E + \varepsilon_0$ is the center-of-mass energy of the projectile.

A. Core recoil model

A special case of the adiabatic model is when the scattering is dominated by the core-target interaction. This is the core recoil model in which the valence-target interaction is neglected. This provides a considerable simplification of the adiabatic Hamiltonian, as the only place that the vector $\boldsymbol{r}$ now appears is in the core-target potential. This dependence can be transformed away using the translation operator

$$U_R(\boldsymbol{x}) = \mathrm{e}^{-\mathrm{i}\boldsymbol{x}\cdot\boldsymbol{K}_{\boldsymbol{R}}}. \tag{8}$$

We have

$$V_{cT}(\boldsymbol{R} - \alpha\boldsymbol{r}) = U_R(\alpha\boldsymbol{r}) V_{cT}(\boldsymbol{R}) U_R^\dagger(\alpha\boldsymbol{r}). \tag{9}$$

Since U_R commutes with $T_{\boldsymbol{R}}$ and the valence potential has been neglected in Eq. (7), the wave function in the core recoil model can be written [2]

$$\langle \boldsymbol{r},\boldsymbol{R}|\Psi_{\boldsymbol{K}}^{\mathrm{ad}(+)}\rangle$$

$$=\langle \boldsymbol{r},\boldsymbol{R}|U_R(\alpha\boldsymbol{r})\frac{\mathrm{i}\epsilon}{E_0^+-T_{\boldsymbol{R}}-V_{cT}(\boldsymbol{R}_{\mathbf{op}})}U_R^{\dagger}(\alpha\boldsymbol{r})|\phi_0,\boldsymbol{K}\rangle$$

$$=\langle \boldsymbol{r},\boldsymbol{R}|U_R(\alpha\boldsymbol{r})\frac{\mathrm{i}\epsilon}{E_0^+-T_{\boldsymbol{R}}-V_{cT}(\boldsymbol{R}_{\mathbf{op}})}\mathrm{e}^{\mathrm{i}\alpha\boldsymbol{r}\cdot\boldsymbol{K}}|\phi_0,\boldsymbol{K}\rangle$$

$$=\phi_0(\boldsymbol{r})\mathrm{e}^{\mathrm{i}\alpha\boldsymbol{r}\cdot\boldsymbol{K}}\langle \boldsymbol{R}-\alpha\boldsymbol{r}|\frac{\mathrm{i}\epsilon}{E_0^+-T_{\boldsymbol{R}}-V_{cT}(\boldsymbol{R}_{\mathbf{op}})}|\boldsymbol{K}\rangle$$

$$=\phi_0(\boldsymbol{r})\mathrm{e}^{\mathrm{i}\alpha\boldsymbol{r}\cdot\boldsymbol{K}}\chi_{\boldsymbol{K}}^{(+)}(\boldsymbol{R}-\alpha\boldsymbol{r}), \tag{10}$$

where $\boldsymbol{R}_{\mathbf{op}}$ is the operator corresponding to the center-of-mass coordinate of the projectile.

Here $\chi_{\boldsymbol{K}}^{(+)}$ is the two-body distorted wave for a particle of mass μ in the core-target potential,

$$\langle \boldsymbol{R}|\chi_{\boldsymbol{K}}^{(+)}\rangle=\langle \boldsymbol{R}|\mathrm{i}\epsilon G_{\mathrm{ad}}^{(+)}|\boldsymbol{K}\rangle, \tag{11}$$

and $G_{\mathrm{ad}}^{(+)}$ is the adiabatic Green's operator with the valence-target potential switched off:

$$G_{\mathrm{ad}}^{(+)}=\frac{1}{E_0^+-T_{\boldsymbol{R}}-V_{cT}(\boldsymbol{R}_{\mathbf{op}})}. \tag{12}$$

The core recoil model wave function, when evaluated in the appropriate few-body T-matrix with the valence-target interaction neglected, allows a factorization into a T-matrix for a point particle of mass μ, multiplied by a formfactor, F_{00} [2]:

$$T_{00}^{\mathrm{ad}}(\boldsymbol{K},\boldsymbol{K}')=\langle \boldsymbol{K}'|V_{cT}|\chi_{\boldsymbol{K}}^{(+)}\rangle F_{00}(\alpha\boldsymbol{Q}), \tag{13}$$

$$F_{00}(\alpha\boldsymbol{Q})=\langle \phi_0|\mathrm{e}^{\mathrm{i}\alpha\boldsymbol{r}\cdot\boldsymbol{Q}}|\phi_0\rangle. \tag{14}$$

The elastic differential cross section can then be obtained from that of a point particle multiplied by the formfactor squared:

$$\left(\frac{\mathrm{d}\sigma}{\mathrm{d}\Omega}\right)_{\mathrm{el}}=\left(\frac{\mathrm{d}\sigma}{\mathrm{d}\Omega}\right)_{\mathrm{point}}|F_{00}(\alpha\boldsymbol{Q})|^2. \tag{15}$$

The point particle elastic cross section is that obtained for a particle of reduced mass μ interacting via the core-target potential, with a center-of-mass energy E_0. The formfactor includes all effects of excitation and breakup of the halo structure.

B. Validity of the adiabatic approximation

The range of validity of the adiabatic approximation has often been investigated by comparison with CDCC calculations which do not make the adiabatic approximation, but instead, use a discretized continuum spectrum of breakup energies for the projectile [7]. By examining the relative excitation and breakup energies required to gain convergence in the CDCC calculations it is found that the adiabatic approximation gives a better estimate of the elastic cross section than one might expect.

TABLE I. Woods-Saxon potential parameters for core-target and core-valence interactions. Energies are in MeV and lengths in fm.

	V	R_V	a_V	W	R_W	a_W
^{10}Be+ ^{12}C	123.00	0.750	0.800	65.00	0.780	0.800
α+ ^{12}C	37.16	1.846	0.452	13.27	1.846	0.452
^{10}Be+n	86.42	1.000	0.530			
α+2n	172.17	0.800	0.300	(ground state)		
α+2n	134.82	0.800	0.728	(d-wave resonance)		

Estimates of the average excitation and breakup energies involved in the scattering of the projectile have been formulated using the core recoil model [8]. The adiabatic approximation is expected to be valid when the collision time of the projectile and target, t_{coll}, is short in comparison to the time associated with the core-valence internal motion, t_{int}. In Ref. [8], an upper limit on the ratio of these times was given as

$$\frac{t_{\mathrm{coll}}}{t_{\mathrm{int}}}<\lambda, \tag{16}$$

where

$$\lambda=2\frac{m_v}{m_c}\frac{m_T}{(m_P+m_T)}\frac{R_0}{a^2}\frac{1}{K}, \tag{17}$$

and R_0 defines the range of the core-target interaction and a the diffuseness. The adiabatic approximation is then expected to be valid when

$$\lambda\ll 1. \tag{18}$$

Note that λ is strongly dependent on the valence-to-core mass ratio, and only weakly dependent on the incident energy of the projectile, through the $1/K$ dependence. Also note that the derivation of λ in Ref. [8] involves an estimate of the excitation energy involved, but the projectile binding energy does not appear.

Using values for the range and diffuseness of the core-target interaction from Table I, some typical values for λ are

$$^{11}\mathrm{Be}+\ ^{12}\mathrm{C}\ \text{ at 10 MeV/nucleon}\Rightarrow\lambda=0.14,$$

$$^{6}\mathrm{He}+\ ^{12}\mathrm{C}\ \text{ at 10 MeV/nucleon}\Rightarrow\lambda=5.$$

These values set upper limits on the time ratio that must be much less than unity. From these values we would expect that when the valence-target interaction is neglected, the adiabatic approximation would give a reasonable description of the exact cross section for ^{11}Be, but a poor description for ^{6}He, at 10 MeV/nucleon.

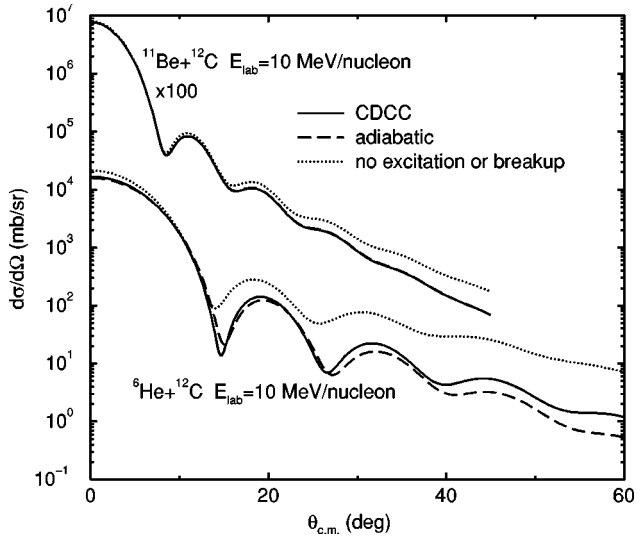

FIG. 1. CDCC (solid) versus adiabatic (dashed) calculations for ^{11}Be and ^{6}He elastic scattering from a ^{12}C target at 10 MeV/nucleon. The valence-target interaction has been neglected as well as the Coulomb interaction. The cross section in the limit of no excitation or breakup is represented by the dotted line. The ^{11}Be cross sections are multiplied by 100.

C. Adiabatic versus CDCC numerical calculations

Extensive studies of deuteron elastic scattering have shown that there is more to the adiabatic approximation than the basic assumption that the excitation energy of the projectile is small in comparison to the center-of-mass energy of the projectile.

Figure 1 compares adiabatic and CDCC calculations for ^{11}Be and ^{6}He elastic scattering from a ^{12}C target at 10 MeV/nucleon. The calculations neglect the valence-target interaction and do not include any Coulomb potential. The adiabatic cross section with the valence-target interaction neglected is just the core recoil model cross section obtained from Eq. (15).

The core-target potential parameters are given in Table I. The ^{10}Be radius parameters are to be multiplied by $10^{1/3}+12^{1/3}$ and the α by $12^{1/3}$.

The ground state wave function of ^{11}Be is assumed to be a pure $2s_{1/2}$ neutron single particle state, with a separation energy of 0.503 MeV, calculated in a central Woods-Saxon potential (Table I). The potential depth is adjusted to obtain the required binding energy of the ^{10}Be$+n$ system. Assuming a core root mean squared (rms) radius of 2.28 fm, this generates the ^{11}Be composite nucleus, with rms radius of 2.90 fm, in agreement with a recent few-body analysis of halo sizes [12,13].

The CDCC calculations were performed using FRESCO [23]. The $1p_{1/2}$ bound state in ^{11}Be, with an excitation energy of 320 keV, was included. The ^{10}Be$+n$ continuum was modeled using 10 bins from 0 to 20 MeV for each of the *s*-, *p*-,*d*-, and *f*-wave breakup states.

A two-body dineutron model was assumed for the ground state wave function of ^{6}He, with a binding energy of 0.975 MeV. The dineutron is assumed to be in a $2s$ single particle state. The $\alpha+2n$ potential used to generate the two-body ground state wave function was assumed to have a Woods-Saxon form (Table I).

The $\alpha+2n$ continuum, due to the breakup of ^{6}He, was modeled using 15 bins from 0 to 30 MeV for each of the *s*-, *p*-, and *f*-wave breakup states, using the same potential as that used for the ground state wave function. The *d*-wave breakup states included a resonance at 1.8 MeV above the ground state, with a bin below the resonance and 15 bins up to 30 MeV above the resonance. A potential which reproduced a 1.8 MeV resonance in $\alpha+2n$ with a width of 113 keV, was used for these *d*-wave breakup states (Table I).

The cross section in the limit of no excitation or breakup is calculated by folding the core-target potential over the ground state wave function to form a two-body projectile-target interaction. This is shown by the dotted line as a reference to highlight the importance of excitation and breakup channels using the different methods.

Figure 1 shows that the effect of the adiabatic assumption is negligible for ^{11}Be and small for ^{6}He, even though the estimate in Sec. II B suggests otherwise. To understand why this is the case, the leading order corrections to the adiabatic approximation are evaluated in the following sections.

III. FIRST ORDER NONADIABATIC CORRECTIONS

Corrections to the adiabatic approximation arise because the scattering process mixes in excited states of the projectile, for which $(H_{vc}+\varepsilon_0)$ is nonzero. Therefore, we expand the wave function of Eq. (5) in powers of $(H_{vc}+\varepsilon_0)$, where to first order we have

$$|\Psi_{\boldsymbol{K}}^{(+)}\rangle \simeq |\Psi_{\boldsymbol{K}}^{\mathrm{ad}(+)}\rangle + G_{\mathrm{ad}}^{(+)}(H_{vc}+\varepsilon_0)|\Psi_{\boldsymbol{K}}^{\mathrm{ad}(+)}\rangle. \quad (19)$$

The first order nonadiabatic correction to the elastic adiabatic *T*-matrix is then

$$\Delta T_{00}^{\mathrm{ad}}(\boldsymbol{K},\boldsymbol{K}') = \langle \Psi_{\boldsymbol{K}'}^{\mathrm{ad}(-)}|(H_{vc}+\varepsilon_0)|\Psi_{\boldsymbol{K}}^{\mathrm{ad}(+)}\rangle. \quad (20)$$

The adiabatic wave function is

$$\Psi_{\boldsymbol{K}}^{\mathrm{ad}(+)}(\boldsymbol{R},\boldsymbol{r}) = \phi_0(\boldsymbol{r})\,\psi_{\boldsymbol{K}}^{\mathrm{ad}(+)}(\boldsymbol{R},\boldsymbol{r}), \quad (21)$$

where $\psi_{\boldsymbol{K}}^{\mathrm{ad}(+)}$ is the distorted wave for the two-body projectile-target scattering system in the potential $V_{cT}(\boldsymbol{R}-\alpha\boldsymbol{r})+V_{vT}(\boldsymbol{R}-\beta\boldsymbol{r})$, with a reduced mass μ, and normalized so that it has an incident plane wave in $\boldsymbol{R}$ with unit amplitude.

The operator product of the three factors $\phi_0(\boldsymbol{r})$, $(H_{vc}+\varepsilon_0)$, and $\phi_0(\boldsymbol{r})$ which appears in Eq. (20) can be expressed as (see the Appendix)

$$\phi_0(\boldsymbol{r})(H_{vc}+\varepsilon_0)\phi_0(\boldsymbol{r}) = -\frac{\hbar^2}{2\mu_{vc}}\boldsymbol{\nabla}_{\boldsymbol{r}}\phi_0^2\cdot\boldsymbol{\nabla}_{\boldsymbol{r}}. \quad (22)$$

This result assumes that ϕ_0 is an *s*-state and, hence, without loss of generality, can be assumed to be real. The result also assumes that V_{vc} is local.

The expression (22) can be conveniently evaluated by allowing the two operators to operate in opposite directions,

i.e., the left del on the bra and the right del on the ket. Thus, the matrix element is reduced to

$$\Delta T_{00}^{\rm ad} = \sum_{\mu=\pm 1,0} (-1)^{\mu} \frac{\hbar^2}{2\mu_{vc}} \times \langle (\boldsymbol{\nabla}_{\boldsymbol{r}})_{\mu} \psi_{\boldsymbol{K}'}^{{\rm ad}(-)}, \phi_0 | \phi_0, (\boldsymbol{\nabla}_{\boldsymbol{r}})_{-\mu} \psi_{\boldsymbol{K}}^{{\rm ad}(+)} \rangle. \quad (23)$$

A. Nonadiabatic corrections to the core recoil model

Using the analytical wave function of the core recoil model, the matrix element for the first order correction to the adiabatic elastic T-matrix can be simplified significantly. By translating the two-body distorted waves,

$$\chi_{\boldsymbol{K}}^{(+)}(\boldsymbol{R}-\alpha\boldsymbol{r}) = U_R \chi_{\boldsymbol{K}}^{(+)}(\boldsymbol{R}), \quad (24)$$

$$(\chi_{\boldsymbol{K}'}^{(-)}(\boldsymbol{R}-\alpha\boldsymbol{r}))^* = (\chi_{\boldsymbol{K}'}^{(-)}(\boldsymbol{R}))^* U_R^{\dagger}, \quad (25)$$

the adiabatic wave functions in the core recoil model can be written as

$$\psi_{\boldsymbol{K}}^{{\rm ad}(+)}(\boldsymbol{R},\boldsymbol{r}) = e^{-i\alpha\boldsymbol{r}\cdot(\boldsymbol{K_R}-\boldsymbol{K})} \chi_{\boldsymbol{K}}^{(+)}(\boldsymbol{R}), \quad (26)$$

$$(\psi_{\boldsymbol{K}'}^{{\rm ad}(-)}(\boldsymbol{R},\boldsymbol{r}))^* = (\chi_{\boldsymbol{K}'}^{(-)}(\boldsymbol{R}))^* e^{i\alpha\boldsymbol{r}\cdot(\boldsymbol{K_R}-\boldsymbol{K}')}. \quad (27)$$

The derivatives with respect to $\boldsymbol{r}$ are now straightforward since the $\boldsymbol{r}$ dependence has been separated. Therefore, when we take the derivative followed by the inner product of Eqs. (26) and (27), the $\boldsymbol{K_R}$ operators in the exponents cancel, allowing the formfactor of Eq. (14) to be factored out. This leaves us with the first order correction to the adiabatic elastic T-matrix:

$$\Delta T_{00}^{\rm ad} = \frac{\hbar^2\alpha^2}{2\mu_{vc}} {\rm X}(\boldsymbol{K},\boldsymbol{K}') F_{00}(\alpha\boldsymbol{Q}), \quad (28)$$

where

$${\rm X}(\boldsymbol{K},\boldsymbol{K}') = \langle \chi_{\boldsymbol{K}'}^{(-)} | (\boldsymbol{K_R}-\boldsymbol{K}')\cdot(\boldsymbol{K_R}-\boldsymbol{K}) | \chi_{\boldsymbol{K}}^{(+)} \rangle. \quad (29)$$

B. Evaluation of the nonadiabatic corrections using the eikonal approximation

In Ref. [19], Eq. (28) was evaluated using the eikonal approximation. This leads to simple formulas for the corrections. Using the eikonal approximation to the distorted waves,

$$\chi_{\boldsymbol{K}}^{(+)}(\boldsymbol{R}) = \exp\left[i\boldsymbol{K}\cdot\boldsymbol{R} - \frac{{\rm i}K}{2E_0}\int_{-\infty}^{z} dz_1 V_{cT}(\boldsymbol{b}+z_1\hat{\boldsymbol{K}}) \right], \quad (30)$$

$$(\chi_{\boldsymbol{K}'}^{(-)}(\boldsymbol{R}))^* = \exp\left[-i\boldsymbol{K}'\cdot\boldsymbol{R} - \frac{{\rm i}K'}{2E_0}\int_{z'}^{\infty} dz_1' V_{cT}(\boldsymbol{b}+z_1'\hat{\boldsymbol{K}}') \right], \quad (31)$$

and by making the small angle approximation, $\hat{\boldsymbol{K}}\cdot\hat{\boldsymbol{K}}' = 1$, which is consistent with the eikonal approximation, Eq. (28) can be written as [19]

$$\Delta T_{00}^{\rm ad} = \langle \chi_{\boldsymbol{K}'}^{(-)} | \Delta V_{cT} | \chi_{\boldsymbol{K}}^{(+)} \rangle F_{00}(\alpha\boldsymbol{Q}), \quad (32)$$

where

$$\Delta V_{cT} = \frac{\gamma}{4E_0}\left((V_{cT})^2 - \int_{-\infty}^{z} dz_1 \boldsymbol{\nabla}_{\boldsymbol{b}} V_{cT}(\boldsymbol{b}+z_1\hat{\boldsymbol{K}}) \cdot \int_{z}^{\infty} dz_2 \boldsymbol{\nabla}_{\boldsymbol{b}} V_{cT}(\boldsymbol{b}+z_2\hat{\boldsymbol{K}}) \right), \quad (33)$$

and γ is the mass ratio

$$\gamma = \frac{m_v}{m_c}\frac{m_T}{(m_P+m_T)}. \quad (34)$$

In evaluating the matrix element in Eq. (32), the eikonal distorted waves combine to form the eikonal phase factor,

$$\chi_{cT}(b) = -\frac{K}{2E_0}\int_{-\infty}^{\infty} dz V_{cT}(\boldsymbol{b}+z\hat{\boldsymbol{K}}), \quad (35)$$

in which the z integration has been performed. Note that this is possible since, for elastic scattering, $K'=K$. The z integration in Eq. (32) therefore only involves ΔV_{cT}, and we can define the quantity

$$\tilde{\chi}(b) = -\frac{K}{2E_0}\int_{-\infty}^{\infty} dz \Delta V_{cT}. \quad (36)$$

For a central potential, the integral over all z of ΔV_{cT} can be simplified to a single integral over all z of the potential squared,

$$\tilde{\chi}(b) = -\frac{\gamma K}{8E_0^2}\left(1 + b\frac{d}{db}\right)\int_{-\infty}^{\infty} dz V_{cT}^2(\sqrt{b^2+z^2}). \quad (37)$$

We can now write Eq. (32) as a scattering amplitude,

$$\Delta f_{00}^{\rm eik} = K\int_0^{\infty} b db J_0(Qb) S(b) \tilde{\chi}(b) F_{00}(\alpha\boldsymbol{Q}). \quad (38)$$

The eikonal scattering amplitude in the core recoil model, including first order nonadiabatic corrections, is then

$$\overline{f}_{00}^{\rm eik} = {\rm i}K\int_0^{\infty} b db J_0(Qb)[1 - S(b)(1+{\rm i}\tilde{\chi})] F_{00}(\alpha\boldsymbol{Q}), \quad (39)$$

where $\overline{f}^{\rm eik}_{00} = f^{\rm eik}_{00} + \Delta f^{\rm eik}_{00}$. Here

$$S(b) = \exp\left[-\frac{iK}{2E_0}\int_{-\infty}^{\infty} dz V_{cT}(\sqrt{b^2+z^2}) \right] \tag{40}$$

is the eikonal S-matrix for ^{11}Be as a point particle moving in the core-target potential.

We see that the nonadiabatic correction term, $\tilde{\chi}$ of Eq. (37), is a dimensionless quantity, whose size relative to unity determines the magnitude of the corrections.

The structure of the expression (37) for the correction factor $\tilde{\chi}$ can be traced to the physical origin of corrections to the adiabatic approximation. In the few-body model used here these corrections arise from excitation of the projectile through tidal forces generated by the interaction of the core with the target. These forces arise because of the displacement of the core from the center-of-mass of the projectile and it is therefore natural that the mass ratio m_v/m_c and derivatives of the core-target potential should be crucial. There is a quadratic dependence on V_{cT} because a two-step process must be involved if the projectile is to end up in the ground state (elastic scattering). The extra $1/E_0$ factor in $\tilde{\chi}$, over and above that expected from the energy dependence of the eikonal phase [see Eqs. (35) and (36)], must be related to the expected dependence on the collision time discussed in Sec. II B.

We note that $\tilde{\chi}$ is multiplied by the eikonal S-matrix which will restrict the impact parameters contributing to the overall corrections.

C. Exact evaluation of nonadiabatic corrections

While the eikonal approximation provides useful insights into the nature of the nonadiabatic corrections, the matrix element in Eq. (29) can be evaluated exactly using a partial wave expansion. The quantity $\mathrm{X}(\boldsymbol{K},\boldsymbol{K}')$, defined in Eq. (29), was shown in Ref. [19] to have the alternative form,

$$\mathrm{X}(\boldsymbol{K},\boldsymbol{K}') = -\langle \chi^{(-)}_{\boldsymbol{K}'} | [\boldsymbol{K}_{\boldsymbol{R}}, V_{cT}] G^{(+)2}_{\rm ad} [\boldsymbol{K}_{\boldsymbol{R}}, V_{cT}] | \chi^{(+)}_{\boldsymbol{K}} \rangle. \tag{41}$$

We can write $\chi^{(+)}_{\boldsymbol{K}}$ as a partial wave sum,

$$\langle \boldsymbol{R} | \chi^{(+)}_{\boldsymbol{K}} \rangle = 4\pi \sum_{\ell m} i^{\ell} Y^{*}_{\ell m}(\hat{\boldsymbol{K}}) Y_{\ell m}(\hat{\boldsymbol{R}}) \chi^{(+)}_{\ell}(R), \tag{42}$$

where $\chi^{(+)}_{\ell}$ is the solution of the radial Schrödinger equation

$$(E_0 - T_{\ell} - V_{cT}) \chi^{(+)}_{\ell}(R) = 0, \tag{43}$$

and T_{ℓ} is radial kinetic energy operator,

$$T_{\ell} = -\frac{\hbar^2}{2\mu}\frac{1}{R}\frac{\mathrm{d}^2}{\mathrm{d}R^2}R + \frac{\hbar^2}{2\mu}\frac{\ell(\ell+1)}{R^2}. \tag{44}$$

The partial distorted wave, $\chi^{(+)}_{\ell}$, has the asymptotic form (ignoring the Coulomb interaction)

$$\chi^{(+)}_{\ell}(R) \underset{R\to\infty}{\sim} \frac{i}{2KR}(H^{(-)}_{\ell} - S_{\ell} H^{(+)}_{\ell}), \tag{45}$$

where S_{ℓ} is the partial wave S-matrix, and $H^{(\pm)}_{\ell}$ are radial Hankel functions, i.e., irregular solutions of the equation

$$\left[\frac{d^2}{dR^2} - \frac{\ell(\ell+1)}{R^2} - \frac{2\mu}{\hbar^2} V + K^2 \right] y_{\ell} = 0. \tag{46}$$

With a similar expression for $\chi^{(-)}_{\boldsymbol{K}'}$ and using a partial wave sum for $G^{(+)}_{\rm ad}$, the matrix element of Eq. (41) can be reduced to [20]

$$\mathrm{X}(\boldsymbol{K},\boldsymbol{K}') = 4\pi \sum_{\ell} P_{\ell}(\cos\theta) \tilde{X}_{\ell}, \tag{47}$$

where we have defined

$$\tilde{X}_{\ell} = \left[(\ell+1) \int_0^{\infty} R^2 dR (\overline{X}^{(+)}_{K,\ell,\ell+1})^2 + \ell \int_0^{\infty} R^2 dR (\overline{X}^{(+)}_{K,\ell,\ell-1})^2 \right]. \tag{48}$$

The nonadiabatic correction to the elastic scattering amplitude in the core recoil model is then

$$\Delta f_{00} = -\gamma F_{00}(\alpha \boldsymbol{Q}) \sum_{\ell} P_{\ell}(\cos\theta) \tilde{X}_{\ell}. \tag{49}$$

In Eq. (48), $\overline{X}^{(+)}_{K\ell\ell'}$ is the solution of the inhomogeneous equation

$$(E_0 - T_{\ell'} - V_{cT}) \overline{X}^{(+)}_{K\ell\ell'}(R) = \frac{dV_{cT}}{dR} \chi^{(+)}_{\ell}(R), \tag{50}$$

with asymptotic form (ignoring the Coulomb interaction)

$$\overline{X}^{(+)}_{K\ell\ \ell'}(R) \underset{R\to\infty}{\sim} \frac{i}{2R} S_{\ell\ \ell'} H^{(+)}_{\ell'}, \tag{51}$$

and where ℓ' can take two values, which leads to the two terms in Eq. (48):

$$\ell' = \ell \pm 1. \tag{52}$$

We have defined $S_{\ell\ \ell'}$ as the coefficient of the Hankel function in the inhomogeneous solution. It can be shown that it is equivalent to the difference between the S-matrix for the homogeneous solutions for ℓ and ℓ',

$$S_{\ell\ \ell'} = \pm(S_{\ell} - S_{\ell'}), \quad \ell' = \ell \pm 1. \tag{53}$$

The oscillatory nature of $\overline{X}^{(+)}_{K\ell\ \ell'}(R)$, for large R, means that the integrals in Eq. (48) have to be dealt with carefully. The asymptotic form for the solutions to the differential equations (43) and (50) is reached when R is outside the range of the potential (V_{cT}). The radial Hankel functions, $H^{(\pm)}_{\ell}$, have the asymptotic form

$$H_\ell^{(\pm)} \underset{R\to\infty}{\sim} e^{\pm i(KR-\ell\pi/2)}, \tag{54}$$

when

$$KR \gg \ell(\ell+1). \tag{55}$$

The solutions of the differential equations were computed out to a radius $R=R_0$, which is outside the range of the potential. Then, the integrals from R_0 to R_ℓ, where R_ℓ is chosen so that the asymptotic condition (55) is met, are performed using the explicit form of the Hankel function [24],

$$H_\ell^{(+)} = e^{iKR}\sum_{s=0}^{\ell} \frac{i^{s-\ell}}{2^s s!}\frac{(\ell+s)!}{(\ell-s)!}(KR)^{-s}. \tag{56}$$

The integral of the asymptotic form of the Hankel function, $H_{\ell'}^{(+)}$, from $R_{\ell'}\to\infty$ can be performed analytically by making the substitution $R=iy+R_{\ell'}$, and integrating over the complex plane,

$$\int_{R_{\ell'}}^{\infty} dR e^{2i(KR-\ell'\pi/2)} = i\int_0^\infty dy e^{-2Ky+2iKR_{\ell'}-i\ell'\pi}$$

$$= \frac{i}{2K}e^{2iKR_{\ell'}-i\ell'\pi}. \tag{57}$$

It is well known that a partial wave sum can be written exactly as an integral over impact parameters [25]. By making the semiclassical correspondence, $\ell=bK$, and assuming the scattering angle is small, the sum over partial waves can be written as [26]

$$\sum_\ell P_\ell(\cos\theta) \to K\int_0^\infty db J_0(Qb). \tag{58}$$

The eikonal equivalent of $\tilde{X}_\ell$ [Eq. (48)] can then be found by substituting this relation into Eq. (49) and comparing it with Eq. (39) to obtain

$$\gamma\tilde{X}_\ell \equiv bS(b)\tilde{\chi}(b), \tag{59}$$

where γ is the mass ratio of Eq. (34), which also appears on the rhs within the correction term, $\tilde{\chi}$. It is then understood that it is the magnitude of either side of Eq. (59) which determines the overall size of the nonadiabatic corrections: it contains the overlap of the correction term with the elastic scattering *S*-matrix, which determines which impact parameters contribute to the cross section.

IV. NUMERICAL RESULTS

A. Application to ^{11}Be+ ^{12}C elastic scattering

Here we examine the nonadiabatic corrections in the core recoil model for ^{11}Be scattering from a ^{12}C target. ^{11}Be is a good example of a single neutron halo nucleus to which the core recoil model can be applied. The interaction between the ^{10}Be core and the target dominates the elastic scattering and it is thus a reasonable first approximation to neglect the neutron-target interaction. The core recoil model was applied to the elastic scattering of ^{11}Be+ ^{12}C at 49.3 MeV/nucleon in Ref. [2]. At this energy we expect the adiabatic approximation to be good, and we therefore calculate the nonadiabatic corrections at 10 MeV/nucleon, where we have calculated the qualitative estimates for the validity of the approximation earlier.

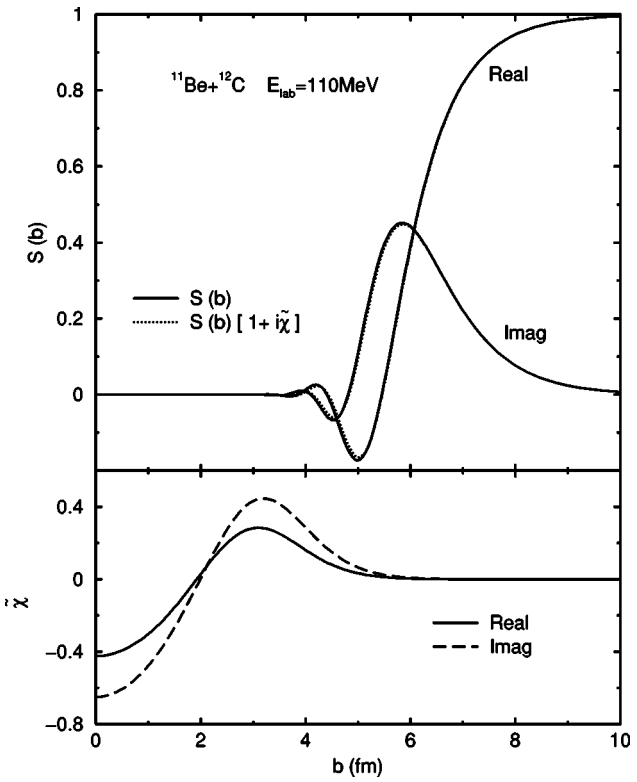

FIG. 2. Eikonal *S*-matrix and nonadiabatic corrections for ^{11}Be+ ^{12}C in the core recoil model. In the top figure, the solid line represents the two-body *S*-matrix for ^{11}Be as a point particle interacting with the ^{12}C target via the core-target interaction. The dotted line includes the first order nonadiabatic corrections through multiplying the *S*-matrix by the factor $(1+i\tilde{\chi})$, while the correction term, $\tilde{\chi}$, is plotted in the bottom figure on the same impact parameter scale.

The potentials and wave functions were discussed in Sec. II C. The potential used for the ^{10}Be core in Ref. [2] was obtained from elastic scattering data at 59.4 MeV/nucleon. Due to the absence of data at lower energies, the same potential will be used at 10 MeV/nucleon, but as the corrections are dependent on the potential geometry, ideally the potential should be fixed by elastic scattering of ^{10}Be at 10 MeV/nucleon.

In Fig. 2 (bottom), the correction term, $\tilde{\chi}$, is plotted against impact parameter for ^{11}Be+ ^{12}C at 10 MeV/nucleon. It has a maximum value of approximately 0.6, which is a significant correction as it is added to unity, but it is then multiplied by the eikonal *S*-matrix, which is plotted on the same impact parameter scale in Fig. 2 (top). We see that the nonadiabatic corrections are largest for small impact parameters, but the *S*-matrix is zero in this region, due to a large

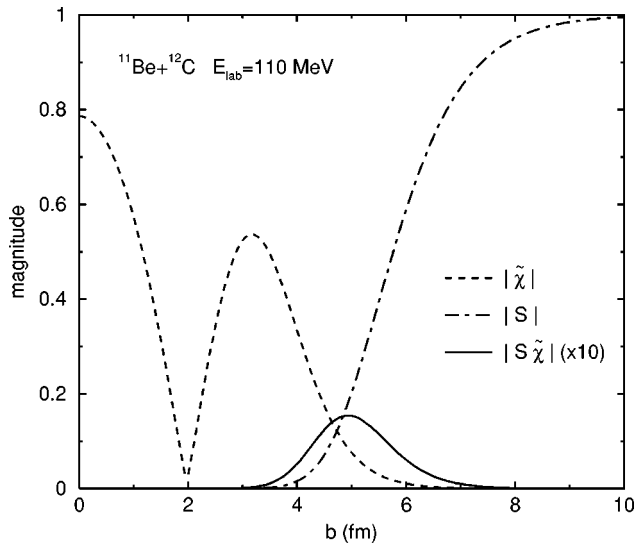

FIG. 3. Overlap of *S*-matrix and nonadiabatic corrections for ^{11}Be+ ^{12}C. The dashed line is the magnitude of the correction term $\tilde{\chi}$ plotted against impact parameter. The dotted-dashed line is the magnitude of the *S*-matrix. The solid line is the magnitude of the product of the *S*-matrix and the correction term $\tilde{\chi}$ multiplied by 10.

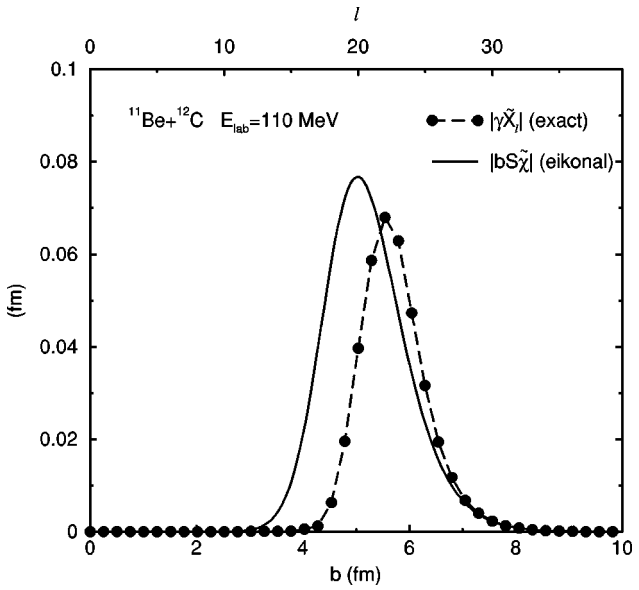

FIG. 4. Exact and eikonal calculations of nonadiabatic corrections for ^{11}Be+ ^{12}C at 10 MeV/nucleon. The solid line represents the eikonal approximation to the nonadiabatic corrections plotted against impact parameter along the bottom axis. It is the overlap of the correction term and the *S*-matrix weighted by the corresponding impact parameter. The circles represent the exact nonadiabatic corrections for each partial wave, which are labeled along the top axis and scaled to match the corresponding impact parameter via the relation $\ell = bK$, where $K = 3.97$ fm^{-1}. The exact correction term, $\tilde{X}_\ell$, is scaled by the mass ratio γ.

imaginary component in the core-target potential. This kills off most of the correction term, with only large impact parameters, corresponding to grazing collisions, contributing to the cross section. The large impact parameters correspond to forward scattering angles where there is little momentum transferred to the projectile during the scattering, and therefore only small corrections to the adiabatic approximation. This can be seen more clearly in Fig. 3, where the magnitude of the *S*-matrix and correction term, $\tilde{\chi}$, is plotted along with the overlap of the two functions (multiplied by 10). It is the maximum size of this overlap, $|S\tilde{\chi}|_{\max}$, in comparison to unity, which determines the overall size of the nonadiabatic corrections. We see that for this system, the maximum value is 0.015, so the nonadiabatic corrections are small.

B. Accuracy of eikonal calculations

The eikonal approximation provides us with an understanding of the nature of the nonadiabatic corrections, but the use of the eikonal approximation must be validated, as in the energy region we are considering, we would expect significant noneikonal corrections.

The nonadiabatic corrections were formulated exactly in Sec. III C; by comparison of the exact nonadiabatic corrections with those calculated in the eikonal approximation, the validity of the eikonal approximation for these calculations can be assessed.

Equation (59) shows that $\gamma\tilde{X}_\ell$ can be compared to the overlap of the correction term and the *S*-matrix in the eikonal approximation, as shown in Fig. 3, multiplied by *b*.

Each side of Eq. (59) is plotted in Fig. 4, with the exact calculation [lhs of Eq. (59)] represented by the circles, and the eikonal calculation [rhs of Eq. (59)] represented by the line. The exact calculation is plotted for each partial wave and scaled to match the corresponding impact parameter for the eikonal calculations. This comparison shows that the overlap of the eikonal *S*-matrix and the correction term, $\tilde{\chi}$, gives a reasonable representation of the nonadiabatic corrections. The corrections are slightly overestimated by the eikonal approximation, especially for the smaller impact parameters, but the larger impact parameters are well reproduced. This is where we expect the eikonal approximation to do better as this corresponds to smaller scattering angles.

In Fig. 5 (top), the differential cross section in the core recoil model is plotted. The two curves represent the different methods of calculating the two-body cross section in the core recoil model. The solid line uses an exact partial wave analysis while the dashed line uses the eikonal approximation; the formfactor is the same in both cases. In the bottom of Fig. 5 the first order nonadiabatic correction is plotted as a fraction of the core recoil cross section. We see that the fractional correction to the adiabatic approximation is well reproduced by the eikonal approximation, even though the eikonal cross section differs significantly from the exact cross section in the core recoil model. The eikonal approximation overestimates the cross section at this energy, but we saw from Fig. 4 that it also overestimates the magnitude of the corrections. As a fraction of the cross section, however, the nonadiabatic corrections are well reproduced. The large core absorption, which kills off most of the corrections, means that only large impact parameters contribute to the cross section, and, therefore, the eikonal approximation gives a reasonable description of the nonadiabatic corrections.

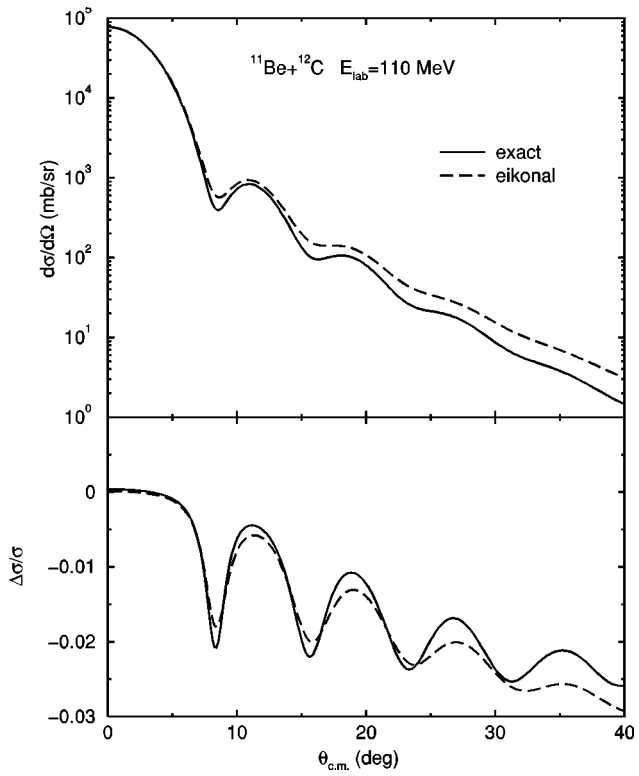

FIG. 5. Angular distribution of the elastic differential cross section for ^{11}Be+ ^{12}C in the core recoil model with no Coulomb interaction. The upper figure compares the cross sections in the core recoil model, using exact (solid) and eikonal (dashed) calculations of the two-body cross section. The lower figure shows the nonadiabatic correction as a fraction of the cross section, with the lines corresponding to exact (solid) and eikonal (dashed) calculations.

We note that the fractional corrections to the adiabatic approximation do not depend on the formfactor, and therefore do not depend on the internal structure of the projectile.

In Sec. II B, an estimate on the accuracy of the adiabatic approximation was given as an upper limit on a time ratio, which had to be much less than one. This upper limit was calculated to be 0.14 for ^{11}Be+ ^{12}C at 10 MeV/nucleon: we then would expect the adiabatic approximation to be good at this energy from this estimate. From the calculations of the first order corrections, the adiabatic approximation is extremely accurate for this system, going beyond the range that the estimate of Sec. II B suggests. This is due to the key role of the strong absorption associated with the scattering at small impact parameters. The maximum overlap function had a value of 0.015 at the peak, which suggests that the adiabatic approximation is approximately ten times better than the estimate of Sec. II B.

C. Application to ^{6}He+ ^{12}C elastic scattering

In the previous section, the ^{11}Be+ ^{12}C system was studied because it was a reasonable approximation to use the core recoil model, as the ratio of the valence-to-core masses was $\frac{1}{10}$. This small ratio also meant that the corrections in this model were small. The large absorption in the ^{10}Be+ ^{12}C potential also played an important role in accuracy of the adiabatic approximation for elastic scattering. To examine the role of the mass ratio and core absorption, the core recoil model was applied to ^{6}He+ ^{12}C elastic scattering.

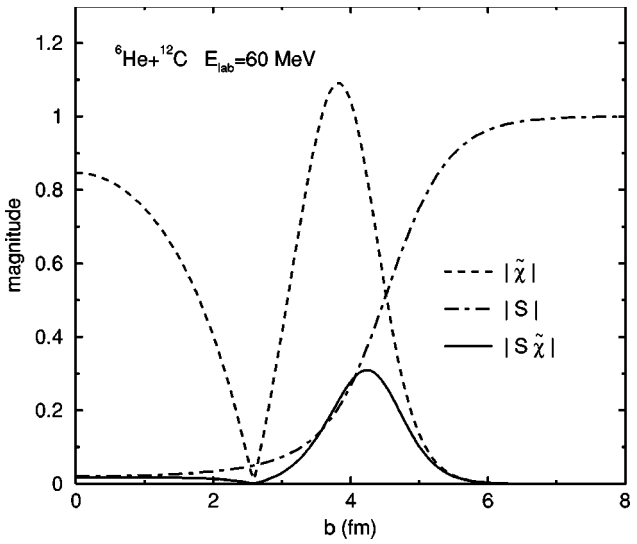

FIG. 6. Overlap of *S*-matrix and nonadiabatic corrections for ^{6}He+ ^{12}C. The dashed line is the magnitude of the correction term $\tilde{\chi}$ plotted against impact parameter. The dotted-dashed line is the magnitude of the *S*-matrix. The solid line is the magnitude of the product of the *S*-matrix and the correction term $\tilde{\chi}$.

The ^{6}He nucleus has a two-neutron halo with an α core, so the ratio of valence-to-core masses is $\frac{1}{2}$. The α core is light and will appear slightly transparent to the ^{12}C target, so corrections at small impact parameters will contribute. Elastic scattering cross sections are available over a wide range of energies for $\alpha+$ ^{12}C, so a more realistic potential can be used. The potentials and wave functions were discussed in Sec. II C.

The magnitude of the nonadiabatic correction term, $\tilde{\chi}$, is plotted in Fig. 6 (dashed line). We see that the $b=0$ value is approximately the same as for ^{11}Be at the same energy. Despite the valence-to-core mass ratio being five times larger for ^{6}He, the smaller $\alpha+$ ^{12}C potential largely cancels this, leaving a correction term similar to that for ^{11}Be. The magnitude of the peak at the potential surface for $\tilde{\chi}$ is larger than its $b=0$ value; for ^{11}Be it was smaller. This is because the $\alpha+$ ^{12}C potential has a sharper potential surface, increasing the derivative of the potential at the surface, thus increasing the correction term [see Eq. (37)]. By comparison with the *S*-matrix (dotted-dashed line), we see that the peak in the correction term now appears in a region of the *S*-matrix which is nonzero; therefore, the overlap with the *S*-matrix is more significant. It has a maximum overlap of around 0.3, compared to 0.015 in the ^{11}Be case. This factor of 20 difference between the two cases arises even though the magnitude of $\tilde{\chi}$ at $b=0$ is of the same order in both cases.

The overlap between the correction term, $\tilde{\chi}$, and the *S*-matrix is increased in the ^{6}He case because the core-target potential has a weaker absorption associated with it. This increases the magnitude of the *S*-matrix in the region of maximum corrections, thus increasing the overlap. Even so, the *S*-matrix is still relatively small at the peak of the correc-

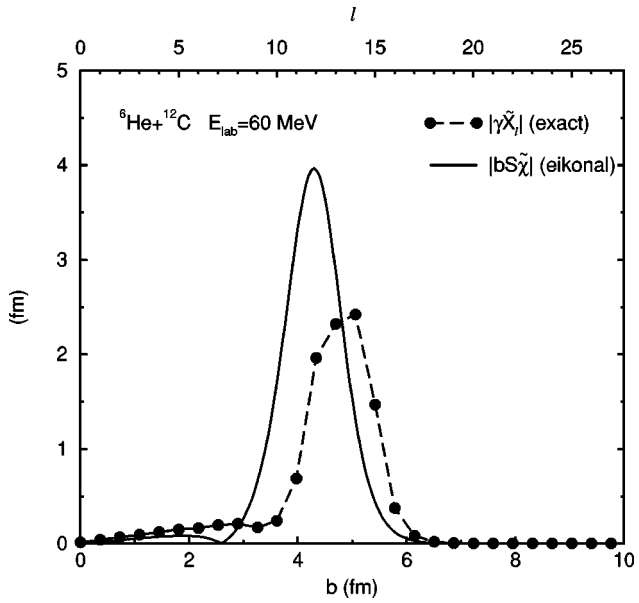

FIG. 7. Exact and eikonal calculations of nonadiabatic corrections for ^{6}He+ ^{12}C at 10 MeV/nucleon. The solid line represents the eikonal approximation to the nonadiabatic corrections plotted against impact parameter along the bottom axis. It is the overlap of the correction term and the *S*-matrix weighted by the corresponding impact parameter. The circles represent the exact nonadiabatic corrections for each partial wave, which are labeled along the top axis and scaled to match the corresponding impact parameter via the relation $\ell = bK$, where $K = 2.77$ fm^{-1}. The exact correction term, $\tilde{X}_\ell$, is scaled by the mass ratio γ.

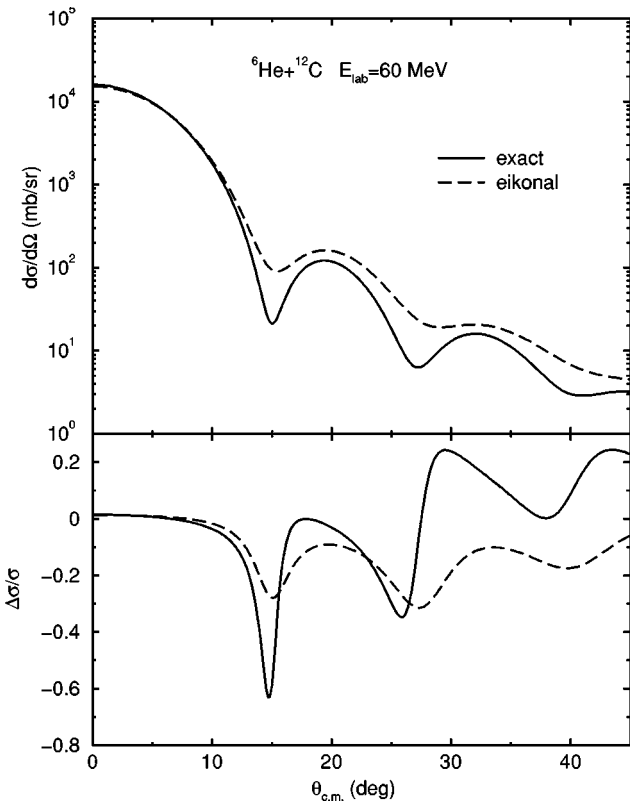

FIG. 8. Angular distribution of the elastic differential cross section for ^{6}He+ ^{12}C in the core recoil model with no Coulomb interaction. The upper figure compares the cross sections in the core recoil model, using exact (solid) and eikonal (dashed) calculations of the two-body cross section. The lower figure shows the nonadiabatic correction as a fraction of the cross section, with the lines corresponding to exact (solid) and eikonal (dashed) calculations.

tion term, $\tilde{\chi}$, and so the maximum overlap is still much smaller than the maximum size of the correction term. The maximum overlap of 0.3 is small in comparison to unity. The corrections to the adiabatic approximation are thus still small, even though the estimate in Sec. II B suggested that the approximation would be poor at this energy.

The accuracy of eikonal calculations for the ^{6}He case is shown in Fig. 7. We see, as in the ^{11}Be case, that the nonadiabatic corrections are overestimated by the eikonal approximation, with the worst agreement for smaller impact parameters. We see in Fig. 8 that this difference is more evident in the fractional correction to the cross section. The *S*-matrix is not as strongly absorbing as for ^{11}Be, so these small impact parameters are contributing to the cross section at large scattering angles. For the largest scattering angles (above 25°), the eikonal approximation to the first order nonadiabatic corrections reduces the cross section, while an exact evaluation shows an increase in the cross section. The eikonal approximation was good for ^{11}Be because the large core absorption meant that only large impact parameters contributed. This is not the case for ^{6}He scattering and so the eikonal approximation is not as accurate.

D. Dependence on core absorption

In the previous section, we see that the nonadiabatic corrections ^{6}He+ ^{12}C at 10 MeV/nucleon are larger than for ^{11}Be+ ^{12}C at the same energy. The reasons for this are twofold: first, the core-to-valence mass ratio is much larger for the former; second, the core-target potential has a smaller imaginary component for the former, due to less absorption of the core. The second effect is examined in more detail here.

The potential we have used for the ^{10}Be+ ^{12}C interaction was obtained at 59.4 MeV/nucleon. As the nonadiabatic corrections have been calculated at the energy of 10 MeV/nucleon, we would expect that the imaginary potential strength to be reduced, but without any experimental data at this energy, its precise value cannot be fixed.

The dependence of the corrections on the imaginary potential strength, W_0, is shown in Fig. 9. The nonadiabatic corrections are plotted for a range of imaginary potential strengths for the ^{11}Be+ ^{12}C reaction at 10 MeV/nucleon. Figure 9 contains three graphs: the top graph plots the modulus of the correction term, $\tilde{\chi}$; the middle figure is the modulus of the *S*-matrix; and the bottom figure is the overlap of the two. The dependence of the corrections on the imaginary potential is shown for various imaginary potential strengths: the solid line represents the 65 MeV imaginary potential that was obtained from the elastic scattering of ^{10}Be+ ^{12}C at 59.4 MeV/nucleon, the dashed line corresponds to a 40 MeV imaginary potential, the dotted line is for $W_0 = 20$ MeV, and the dotted-dashed line represents $W_0 = 10$ MeV.

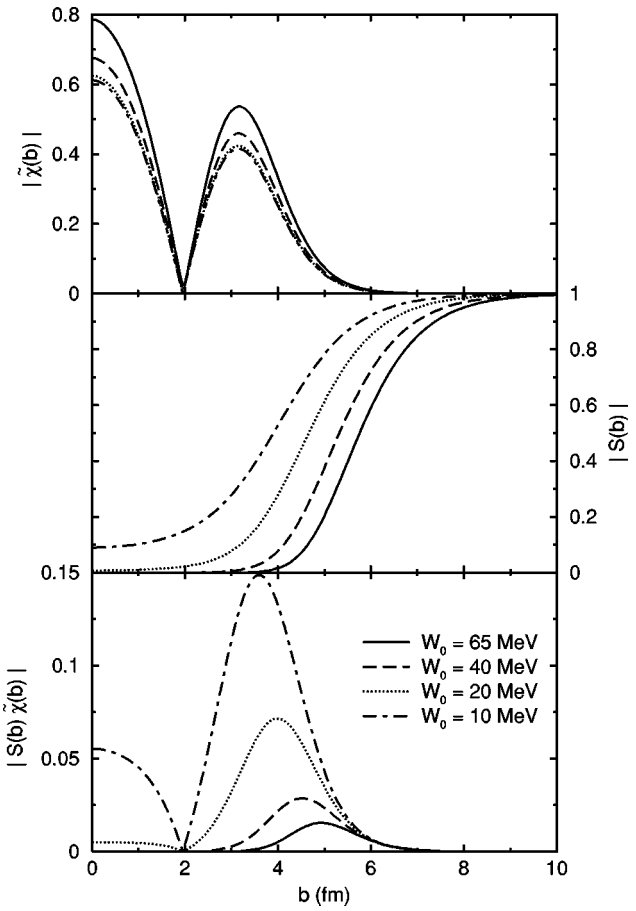

FIG. 9. Nonadiabatic correction term for ^{11}Be+ ^{12}C at 10 MeV/nucleon for varying imaginary potential depths. The top figure plots the modulus of the correction term, $\tilde{\chi}$, versus impact parameter while the middle figure shows the modulus of the *S*-matrix on the same impact parameter scale. The bottom figure is the overlap of the *S*-matrix and $\tilde{\chi}$. The imaginary potential depths for the core-target potential are given in the legend.

We see that different imaginary potential strengths do not affect the correction term $\tilde{\chi}$ significantly, but the effect on the *S*-matrix is large. As the imaginary potential strength is reduced, the correction term, $\tilde{\chi}$, is reduced slightly; but, the target appears more transparent and so the *S*-matrix is increased significantly for the small impact parameters. The overlap of the correction term with the *S*-matrix is then significantly increased, as shown in the bottom figure, and it is this overlap which determines the overall size of the corrections.

The accuracy of the eikonal approximation for evaluating the nonadiabatic corrections was shown to be suspect for ^{6}He, which was said to be due to the weak imaginary potential. To see this effect for the ^{11}Be case, the 20 MeV imaginary potential was used to compare the exact and eikonal calculations of the nonadiabatic corrections. The fractional non-adiabatic corrections are shown in Fig. 10. We see here that the eikonal approximation reproduces the exact corrections poorly for large scattering angles (above 20°), as in the ^{6}He case. The eikonal approximation fails to predict the increase in the cross section for large scattering angles that was

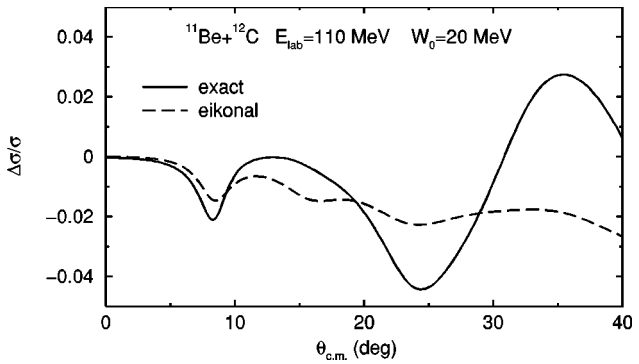

FIG. 10. Angular distribution of the elastic differential cross section for ^{11}Be+ ^{12}C in the core recoil model with the imaginary potential depth reduced to 20 MeV. The nonadiabatic corrections are plotted as a fraction of the cross section, with the lines corresponding to exact (solid) and eikonal (dashed) calculations.

seen when the exact nonadiabatic corrections were included. The nonadiabatic corrections for ^{11}Be are still small compared to the ^{6}He calculations, even when the imaginary potential depth is reduced, due to the smaller valence-to-core mass ratio.

V. IMPROVED ESTIMATE FOR VALIDITY OF ADIABATIC APPROXIMATION

We have shown in our numerical evaluation of the nonadiabatic corrections that strong core absorption improves the accuracy of the adiabatic approximation, going beyond that expected from the estimates of Sec. II B.

The key point is that when strong absorption is present, it is the value of the correction term, $\tilde{\chi}$ [Eq. (37)], in the region near the strong absorption radius which is of importance. The size of the nonadiabatic correction is determined by the maximum overlap of $\tilde{\chi}$ and the *S*-matrix. If $\tilde{\chi}$ is modeled by an exponential and the *S*-matrix by a Woods–Saxon, then a good estimate for the size of the nonadiabatic corrections is $\tilde{\chi}$, evaluated at the strong absorption radius, multiplied by $\frac{1}{2}$ (the value of the *S*-matrix at the strong absorption radius).

We can estimate the value of $\tilde{\chi}$ [Eq. (37)] at the strong absorption radius as the potential in this region has the form of a simple exponential, so that

$$\int_{-\infty}^{\infty} dz V_{cT}^2(\sqrt{b^2+z^2}) = \int_{-\infty}^{\infty} dz V_0^2 e^{-2\sqrt{b^2+z^2}/a}, \quad (60)$$

where a is the diffuseness of the core-target interaction. Since the most important values in the z integral are those around $z=0$, the square root can be expanded in powers of z/b:

$$\int_{-\infty}^{\infty} dz V_0^2 e^{-2\sqrt{b^2+z^2}/a} \approx \int_{-\infty}^{\infty} dz V_0^2 e^{-2b(1+z^2/2b^2)/a}. \quad (61)$$

The integral of the square of the potential can therefore be written

$$\int_{-\infty}^{\infty} dz V_{cT}^2(\sqrt{b^2+z^2}) \approx \sqrt{ba\pi} V_{cT}^2(b), \tag{62}$$

and an estimate of $\tilde{\chi}$, near the strong absorption radius, is

$$\tilde{\chi}(b) \approx \frac{\gamma K}{8E_0^2}\sqrt{a\pi}\,\frac{d}{db} b^{3/2} V_{cT}^2(b). \tag{63}$$

The derivative of the potential dominates in $(d/db)b^{3/2}V_{cT}^2(b)$, and as the potential only depends on b, the overlap of the correction term and the S-matrix at the strong absorption radius can be written

$$|S\tilde{\chi}|_{\max} \approx \frac{\gamma K}{16E_0^2}\sqrt{\pi a} R_s^{3/2} \frac{d}{dR} V_{cT}^2(R)\bigg|_{R=R_s}, \tag{64}$$

where R_s is the strong absorption radius, and γ is the mass ratio in Eq. (34). The adiabatic approximation, for scattering systems with strong core absorption, is then valid when

$$|S\tilde{\chi}|_{\max} \ll 1. \tag{65}$$

For strong absorbing systems, this criterion replaces condition (18).

Equation (64) gives approximate values for $|S\tilde{\chi}|_{\max}$ of 0.01 and 0.2 for ^{11}Be and ^{6}He, respectively. This compares well with calculated values of 0.015 and 0.3 from Figs. 3 and 6. These values greatly improve on the estimates given in Sec. II B, and give the maximum overlap to the correct order of magnitude for scattering systems with core absorption.

VI. SUMMARY

We have calculated first order nonadiabatic corrections for the first time using the core recoil model, in which the valence-target interaction is neglected. Two reactions were studied: the elastic scattering of ^{11}Be and ^{6}He from a ^{12}C target at 10 MeV/nucleon. The nonadiabatic corrections were compared to previous qualitative estimates of the validity of the adiabatic approximation.

The eikonal approximation was used to gain insights into the nature of the nonadiabatic corrections. They were found to be dependent on the overlap of a correction term [Eq. (37)] and the S-matrix. The correction term was found to be strongly dependent on the ratio of the valence mass to that of the core, as with the qualitative estimates. Along with the expected energy dependence, there was also a dependence on the strength and diffuseness of the core-target interaction. The overlap of the correction term with the S-matrix was strongly dependent on the strength of the imaginary potential for the core-target interaction. Strong core absorption kills of most of the nonadiabatic corrections as the maximum of the correction term lies in a region where the S-matrix is zero, while smaller imaginary potentials increase the overlap of the of the S-matrix with the correction term producing larger nonadiabatic corrections. The corrections calculated are much smaller than what is expected from qualitative estimates due to the key role that core absorption plays.

An improved estimate for the validity of the adiabatic approximation, when the valence-target interaction is neglected, is given in Sec. V, which includes the role of core absorption. This new estimate recognizes that when the core-target absorption is strong, it is the size of the correction term in the region near the strong absorption radius which is of importance in determining the size of the nonadiabatic corrections. Equation (64) gives a value which is of the correct order of magnitude for the size of the nonadiabatic corrections when core absorption is present.

In the core recoil model we have used here, nonadiabatic corrections can only arise through projectile excitations occurring from recoil of the core in its scattering by the target. If the valence-target interaction were included, corrections could also arise through recoil of the valence particle. The strong dependence on the valence-to-core mass ratio is then expected to be of great importance in the contribution from these different processes. The corrections for ^{11}Be, although being very small partly due to the small valence-to-core mass ratio, could be much larger when valence particle recoil is included. This will be dealt with elsewhere [20,21].

ACKNOWLEDGMENTS

The authors would like to thank Professor I. J. Thompson and Professor J. A. Tostevin for useful discussions and help in running FRESCO, and J.A.T. for supplying numerical routines. This work is supported by the United Kingdom Engineering and Physical Sciences Research Council (EPSRC) through Grant No. GR/M82141. The financial support of EPSRC (for N.C.S.) is also gratefully acknowledged.

APPENDIX: OPERATOR IDENTITY

We are interested in the operator product of the three factors $\psi^*(\boldsymbol{r})$, $(H-\varepsilon)$, and $\phi(\boldsymbol{r})$. Our result is that this can be reexpressed as

$$\psi^*(H-\varepsilon)\phi(\boldsymbol{r}) = -\frac{\hbar^2}{2\mu}\boldsymbol{\nabla}_{\boldsymbol{r}}\psi^*\phi\cdot\boldsymbol{\nabla}_{\boldsymbol{r}} + \frac{\hbar^2}{2\mu}[(\boldsymbol{\nabla}_{\boldsymbol{r}}\psi^*)\phi - \psi^*(\boldsymbol{\nabla}_{\boldsymbol{r}}\phi)]\cdot\boldsymbol{\nabla}_{\boldsymbol{r}}. \tag{A1}$$

The result assumes that ϕ is an eigenstate of $H = -(\hbar^2/2\mu)\nabla_r^2 + V$ with eigenvalue ε, but ψ can be arbitrary. V must be a local operator. ϕ and ψ do not have to be bound states.

For an s-wave state ϕ in a real potential, ϕ can be assumed to be real and the last term in Eq. (A1) vanishes if $\psi = \phi$:

$$\phi(r)(H-\varepsilon)\phi(r) = -\frac{\hbar^2}{2\mu}\boldsymbol{\nabla}_{\boldsymbol{r}}(\phi)^2\cdot\boldsymbol{\nabla}_{\boldsymbol{r}}. \tag{A2}$$

In proving Eq. (A1), we use round brackets to indicate when the $\boldsymbol{\nabla}$ operator acts only locally on the functions inside the brackets. We have

$$\boldsymbol{\nabla}_{\boldsymbol{r}}\psi^*\phi\cdot\boldsymbol{\nabla}_{\boldsymbol{r}}=(\boldsymbol{\nabla}_{\boldsymbol{r}}\psi^*\phi)\cdot\boldsymbol{\nabla}_{\boldsymbol{r}}+(\psi^*\phi)\nabla_r^2. \tag{A3}$$

By considering the operation of ∇_r^2 on the product of ϕ and an arbitrary function χ,

$$(\nabla_r^2\phi\chi)=(\nabla_r^2\phi)\chi+\phi(\nabla_r^2\chi)+2(\boldsymbol{\nabla}_{\boldsymbol{r}}\phi)\cdot(\boldsymbol{\nabla}_{\boldsymbol{r}}\chi), \tag{A4}$$

Eq. (A3) can be rewritten as

$$\begin{aligned}\boldsymbol{\nabla}_{\boldsymbol{r}}\psi^*\phi\cdot\boldsymbol{\nabla}_{\boldsymbol{r}}&=(\boldsymbol{\nabla}_{\boldsymbol{r}}\psi^*\phi)\cdot\boldsymbol{\nabla}_{\boldsymbol{r}}\\&\quad+\psi^*[\nabla_r^2\phi-(\nabla_r^2\phi)-2(\boldsymbol{\nabla}_{\boldsymbol{r}}\phi)\cdot\boldsymbol{\nabla}_{\boldsymbol{r}}]\\&=[(\boldsymbol{\nabla}_{\boldsymbol{r}}\psi^*)\phi-\psi^*(\boldsymbol{\nabla}_{\boldsymbol{r}}\phi)]\cdot\boldsymbol{\nabla}_{\boldsymbol{r}}\\&\quad+\psi^*\nabla_r^2\phi-\psi^*(\nabla_r^2\phi)\\&=[(\boldsymbol{\nabla}_{\boldsymbol{r}}\psi^*)\phi-\psi^*(\boldsymbol{\nabla}_{\boldsymbol{r}}\phi)]\cdot\boldsymbol{\nabla}_{\boldsymbol{r}}\\&\quad+\psi^*\nabla_r^2\phi-\psi^*\frac{2\mu}{\hbar^2}((V-\varepsilon)\phi),\end{aligned} \tag{A5}$$

where we have put double brackets around the last factor to emphasize that V acts on ϕ only. We can drop these brackets if V is a local operator.

The last line in Eq. (A5) can now be reexpressed in terms of H and we obtain

$$\begin{aligned}\boldsymbol{\nabla}_{\boldsymbol{r}}\psi^*\phi\cdot\boldsymbol{\nabla}_{\boldsymbol{r}}&=[(\boldsymbol{\nabla}_{\boldsymbol{r}}\psi^*)\phi-\psi^*(\boldsymbol{\nabla}_{\boldsymbol{r}}\phi)]\cdot\boldsymbol{\nabla}_{\boldsymbol{r}}\\&\quad-\frac{2\mu}{\hbar^2}\psi^*\left[-\frac{\hbar^2}{2\mu}\nabla_r^2+V-\varepsilon\right]\phi\\&=[(\boldsymbol{\nabla}_{\boldsymbol{r}}\psi^*)\phi-\psi^*(\boldsymbol{\nabla}_{\boldsymbol{r}}\phi)]\cdot\boldsymbol{\nabla}_{\boldsymbol{r}}\\&\quad-\frac{2\mu}{\hbar^2}\psi^*(H-\varepsilon)\phi.\end{aligned} \tag{A6}$$

This is equivalent to the identity given in Eq. (A1).

The identity (A2) is frequently seen in a form which is equivalent to it when $\phi(r)$ is nodeless:

$$H-\varepsilon=-\frac{\hbar^2}{2\mu}\phi^{-1}\boldsymbol{\nabla}_{\boldsymbol{r}}\phi^2\cdot\boldsymbol{\nabla}_{\boldsymbol{r}}\phi^{-1}=\frac{\boldsymbol{A}^{(+)}.\boldsymbol{A}^{(-)}}{2\mu}, \tag{A7}$$

where

$$\boldsymbol{A}^{(+)}=\phi^{-1}\boldsymbol{p}\phi, \tag{A8}$$

$$\boldsymbol{A}^{(-)}=\phi\boldsymbol{p}\phi^{-1}, \tag{A9}$$

and $\boldsymbol{p}=-i\hbar\boldsymbol{\nabla}_{\boldsymbol{r}}$ is the momentum operator. The factorized form (A7) is used in one-dimension in the formulation of super-symmetric quantum mechanics [27].

[1] R.C. Johnson and P.J.R. Soper, Phys. Rev. C **1**, 976 (1970).
[2] R.C. Johnson, J.S. Al-Khalili, and J.A. Tostevin, Phys. Rev. Lett. **79**, 2771 (1997).
[3] J.A. Tostevin *et al.*, Phys. Lett. B **424**, 219 (1998).
[4] J.A. Tostevin, S. Rugmai, and R.C. Johnson, Phys. Rev. C **57**, 3225 (1998).
[5] P. Banerjee, I.J. Thompson, and J.A. Tostevin, Phys. Rev. C **58**, 1042 (1998).
[6] P. Banerjee, J.A. Tostevin, and I.J. Thompson, Phys. Rev. C **58**, 1337 (1998).
[7] M. Yahiro, Y. Iseri, H. Kameyama, M. Kamimura, and M. Kawai, Prog. Theor. Phys. Suppl. **89**, 32 (1986).
[8] R. C. Johnson, in *Proceedings of the European Conference on Advances in Nuclear Physics and Related Areas*, Thessaloniki, Greece, 1997, edited by D. M. Brink, M. E. Grypeos, and S. E. Massen (Giahoudi-Giapouli, Thessaloniki, 1999), p. 297.
[9] R. J. Glauber, in *Lectures in Theoretical Physics*, edited by W. E. Brittin (Interscience, New York, 1959), Vol. 1, p. 315.
[10] J.S. Al-Khalili and R.C. Johnson, Nucl. Phys. **A546**, 622 (1992).
[11] J.S. Al-Khalili, I.J. Thompson, and J.A. Tostevin, Nucl. Phys. **A581**, 331 (1995).
[12] J.S. Al-Khalili, J.A. Tostevin, and I.J. Thompson, Phys. Rev. C **54**, 1843 (1996).
[13] J.S. Al-Khalili and J.A. Tostevin, Phys. Rev. Lett. **76**, 3903 (1996).
[14] J.S. Al-Khalili, J.A. Tostevin, and J.M. Brooke, Phys. Rev. C **55**, R1018 (1997).
[15] J.M. Brooke, J.S. Al-Khalili, and J.A. Tostevin, Phys. Rev. C **59**, 1560 (1999).
[16] H. Amakawa, S. Yamaji, A. Mori, and K. Yazaki, Phys. Lett. **82B**, 13 (1979).
[17] I. J. Thompson, computer program ADIA, Daresbury Laboratory Report, 1984 (unpublished).
[18] J.A. Christley, J.S. Al-Khalili, J.A. Tostevin, and R.C. Johnson, Nucl. Phys. **A624**, 275 (1997).
[19] R.C. Johnson, J. Phys. G **24**, 1583 (1998).
[20] N. C. Summers, Ph.D. thesis, University of Surrey, 2001.
[21] N. C. Summers, R. C. Johnson, and J. S. Al-Khalili (to be submitted).
[22] W. Glöckle, in *Scattering*, edited by R. Pike and P. Sabatier (Academic, London, 2002), Vol. 2, Chap. 3.1.2.
[23] I.J. Thompson, Comput. Phys. Rep. **7**, 167 (1988).
[24] A. Messiah, *Quantum Mechanics* (North-Holland, Amsterdam, 1970), Vol. 1, translated from the French by G. M. Temmer.
[25] J. S. Al-Khalili and J. A. Tostevin, in *Scattering* (Ref. [22]), Vol. 2, Chap. 3.1.3.
[26] J. J. Sakurai, *Modern Quantum Mechanics* (Addison-Wesley, Reading, MA, 1994) (revised ed.).
[27] C.V. Sukumar, J. Phys. A **18**, 2917 (1985).